

# Overview of PLL methods for Distributed Generation units

Bart Meersman, Jeroen De Kooning, Tine Vandoorn, Lieven Degroote, Bert Renders and Lieven Vandevelde

Electrical Energy Laboratory (EELAB),

Department of Electrical Energy, Systems and Automation (EESA),  
Ghent University, Sint-Pietersnieuwstraat 41, B-9000 Ghent, Belgium,

Phone: +32 9 264 34 42, Fax: +32 9 264 35 82

e-mail: Bart.Meersman@UGent.be

**Abstract**—Distributed energy resources are increasingly being connected to the utility grid by means of an inverter. The basic information necessary for these inverter-connected distribution units are the frequency and phase angle of the utility grid. The phase angle can be estimated using phase-locked loops (PLLs). Voltage unbalance, harmonics and other kinds of undesirable perturbations are common conditions in the electric utility which are detrimental for the operation of the PLL. In this paper, three commonly known PLL methods are discussed: the single-phase synchronous reference frame (SRF) PLL, the three-phase SRF PLL and the double SRF PLL. The effect of voltage unbalance on those PLL methods will be discussed in this paper.

**Index Terms**—distributed generation, phase-locked loop (PLL), three-phase voltage-source inverter (VSI), voltage unbalance

## I. INTRODUCTION

Nowadays, distributed energy resources (DER) with photovoltaic systems, wind turbines and combined heat and power installations are increasingly connected to the utility grid by means of an inverter. The frequency and phase angle of the utility voltage represent the basic information for these inverter-connected distribution units and are used for determining the reference value of the injected current. The phase-angle can be estimated using open-loop and closed-loop methods. The closed-loop methods are commonly known as phase-locked loops (PLLs). The quality of lock directly effects the performance of the control loops. Line notches, voltage unbalance, voltage dips, harmonics and other kinds of undesirable perturbations are common conditions faced by the equipment interfaced with the electric utility. These perturbations are detrimental for the operation of the PLL [1]. It is thus important that a robust grid synchronization technique that is able to track the phase angle of the grid voltage is obtained. In this paper, three commonly known PLL methods [1] are studied: the single-phase synchronous reference frame PLL (SRF PLL) [2], the three-phase SRF PLL [3]–[5] and the double synchronous reference frame PLL (double SRF PLL) [6].

## II. SYNCHRONOUS REFERENCE FRAME PLL

A commonly used method in three-phase systems is the SRF method. In this method, the instantaneous phase angle  $\theta$  is detected by synchronizing the PLL rotating reference frame to the utility voltage vector. The reference is locked to the

utility voltage vector phase angle by means of a PI controller which sets the direct axis reference voltage to zero. In single-phase applications, the direct and quadrature axis reference voltage vector need to be constructed.

### A. Single-phase applications

The general principle of the SRF method for single-phase applications is depicted in Fig. 1, the hatted letters denote the estimated variables, small letters the measured variables (eg.  $v_{in}$ ,  $\theta$ ). This algorithm uses two virtual phases which are constructed by the two-phase generator. These two phases will be used for estimating the amplitude, frequency and phase angle of the input voltage, the detection is done by the phase controller.

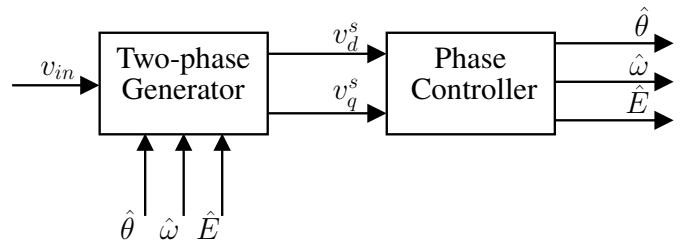


Fig. 1. General principle of a single-phase synchronous reference frame PLL

1) *Two-phase generator*: Several possibilities exist for the two-phase generator, such as a method using a look-up table, a method using the estimated phase angle and amplitude etc. Based on the results which are described in [2], the methods using a first-order and a second-order filter give the best results. The method using the first-order filter shows the shortest estimation time and the method using the second-order filter shows less oscillation [2]. The method using the first-order filter will be implemented in a 16-bit digital signal processor DSP56F8367 of Motorola.

### First-order filter

In Fig. 2,  $v_d^s$  and  $v_q^s$  are obtained by using a first-order low-pass filter [2]. When the input  $v_{in}$  passes the first-order low-pass filter, where the cutoff frequency  $\omega_c$  has the same value

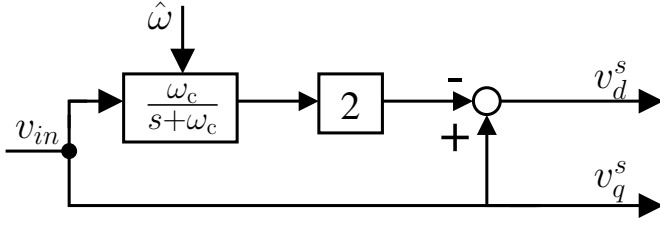


Fig. 2. Method using first-order filter

as the estimated frequency  $\hat{\omega}$  and  $\omega = \hat{\omega}$ ,  $\frac{E}{\sqrt{2}} \sin(\omega t - \frac{\pi}{4})$  is obtained. Therefore,  $v_d^s$  is:

$$v_d^s \cong E \sin(\omega t) - 2 \frac{E}{\sqrt{2}} \sin(\omega t - \frac{\pi}{4}) = E \cos(\omega t) \quad (1)$$

2) *Phase controller*: The phase controller can be implemented using two different methods: a method using the arctangent function or the method using the synchronous frame. The second method, using synchronous frame, delivers the best results [2] and is therefore used in this paper. The method using arctangent function is easy to understand but has implementation difficulties in calculating the arctangent function.

### Synchronous frame

In Fig. 3,  $v_d^s$  and  $v_q^s$  are converted to synchronous reference

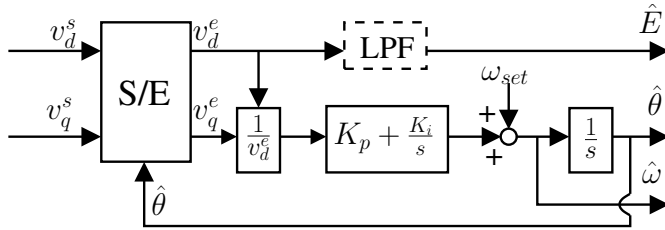


Fig. 3. Method using second-order filter

frame:

$$v_d^e = v_d^s \cos(\hat{\theta}) + v_q^s \sin(\hat{\theta}) \quad (2)$$

$$v_q^e = -v_d^s \sin(\hat{\theta}) + v_q^s \cos(\hat{\theta}) \quad (3)$$

Substituting  $v_d^s = E \cos(\theta)$ ,  $v_q^s = E \sin(\theta)$  into (2) and (3), when the difference  $\hat{\theta} - \theta$  is sufficiently small, the following approximation can be used:

$$v_d^e = E \cos(\hat{\theta} - \theta) \cong E \quad (4)$$

$$v_q^e = E \sin(\hat{\theta} - \theta) \cong E(\hat{\theta} - \theta) \quad (5)$$

$v_d^e$  thus expresses the estimated amplitude  $\hat{E}$ , while  $v_q^e$  expresses the estimated phase-angle error.  $\Delta\omega$  is obtained by controlling the estimated phase-angle error using the PI loop, where  $v_q^e$  is divided by the estimated amplitude  $\hat{E}$ .  $K_p$  and  $K_i$  denote the gains of the PI loop filter.  $\Delta\omega$  is then added to the initial value  $\omega_{set}$  to obtain the estimated frequency  $\hat{\omega}$  and estimated phase angle  $\hat{\theta}$ . Adding  $\omega_{set}$  to  $\Delta\omega$  helps to decrease

the starting time of the PLL. In case of a lot of noise, a LPF can be inserted to reduce the effect of the noise.

### B. Three-phase applications

In three-phase applications, the utility voltage can be expressed in a stationary reference frame which can then be rewritten in a synchronous reference frame. This results in  $v^d$  and  $v^q$  which can be used to estimate the frequency, phase angle and amplitude of the input voltage. The general principle of the three-phase SRF PLL is depicted in Fig. 4. The input voltages  $v_a$ ,  $v_b$  and  $v_c$  are first transformed to the stationary reference frame  $(v_\alpha, v_\beta)$  by means of the following matrix:

$$T = \frac{2}{3} \begin{bmatrix} 1 & -\frac{1}{2} & -\frac{1}{2} \\ 0 & -\frac{\sqrt{3}}{2} & \frac{\sqrt{3}}{2} \end{bmatrix} \quad (6)$$

Fig. 4 could be extended by adding  $\omega_{set}$  to the output of the PI controller to obtain a faster start up.

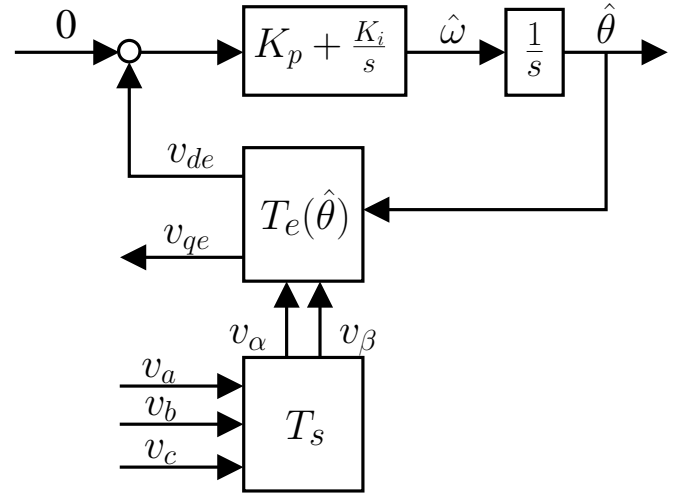


Fig. 4. Block diagram of the three-phase synchronous reference frame PLL

In [4], a proper design method of this three-phase PLL is discussed, the most important aspects are here briefly repeated. The linearised model of the system described in Fig. 4 is depicted in Fig. 5. The closed loop transfer function of this system can be represented as:

$$H_c(s) = \frac{\hat{\Theta}(s)}{\Theta(s)} = \frac{K_f(s) E}{s + K_f(s) E} \quad (7)$$

where  $\hat{\Theta}(s)$  and  $\Theta(s)$  denote the Laplace transform of  $\hat{\theta}$  and  $\theta$  respectively. There are various methods to design the loop filter. In [4], a proportional-integral (PI) loop filter for the second-order loop is used:

$$K_f(s) = K_p \left( \frac{1 + s \tau}{s \tau} \right) \quad (8)$$

where  $K_p$  denotes the gain and  $\frac{1}{\tau}$  the zero of the PI loop filter. In the design of the loop filter, it is desirable that the dynamic performance should satisfy the fast tracking and good filtering characteristics. However, both requirements cannot be satisfied simultaneously because the two conditions are inconsistent.

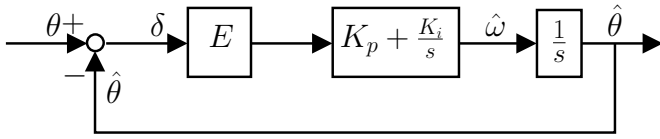


Fig. 5. Linearised model of the three-phase synchronous reference frame PLL

Therefore, a trade-off is required in the design. Under ideal utility conditions, a high bandwidth of the feedback loop yields a fast and precise detection of the phase and amplitude of the utility voltage vector. In case the utility voltage is distorted with high-order harmonics, the SRF-PLL can operate satisfactory if its bandwidth is reduced in order to reject and cancel out the effect of these harmonics on the output. The PLL bandwidth reduction is not an acceptable solution in the presence of unbalanced grid voltages. The stated problem can be solved by adding a simple low-pass filter. These changes can improve the response but the SRF technique suffers from three critical limitations:

- 1) only an approximation but not the true amplitude and phase angle of the positive-sequence component is detected;
- 2) the detected positive-sequence voltages are distorted;
- 3) the dynamic response of the system is significantly reduced.

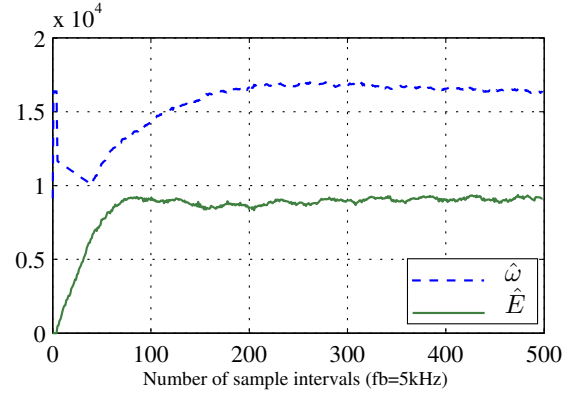
### C. Experimental results

The single-phase and three-phase SRF method were implemented based on [2] and [3] respectively by using a 16-bit digital signal processor by Motorola (DSP56F8367). To evaluate the performance of both PLL methods, several tests were conducted by using a three-phase system. The single-phase SRF method was implemented for each phase. The sample frequency of the three- and single-phase methods was 5 kHz.

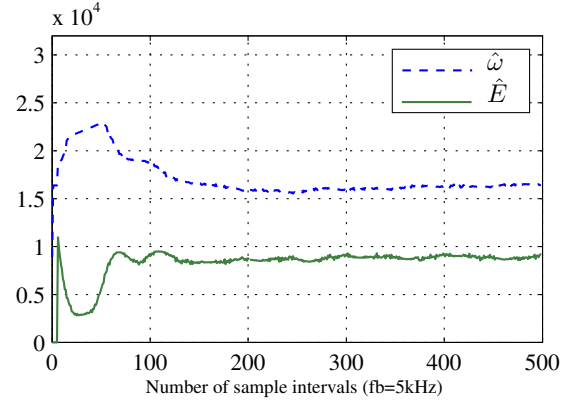
1) *Start up*: In the first test, the dynamic response of both methods was tested. Fig. 6(a) and Fig. 6(b) depict the estimated amplitude and the estimated pulsation of the input voltage of both methods.  $\hat{\omega}$  and  $\hat{E}$  depicted in Fig. 6(b) correspond to phase a. The three single-phase methods started with the same initial conditions, in Fig. 7(b) it can be seen that the three voltages start at zero and converge to the input voltages. Changing the initial conditions (eg.  $\theta_a = 0$ ,  $\theta_b = 120^\circ$  and  $\theta_c = 240^\circ$ ) will have an impact on the convergence time and the dynamic response can be improved. In this test the worst start up was simulated.

The phase voltages are depicted in Fig. 7(a). The estimated voltages of the three-phase method have a better waveform compared to the single-phase method (Fig. 7(b)).

2) *Three-phase symmetrical voltages in steady-state*: In the second test, the ability to obtain the correct phase angle and amplitude was verified. A three-phase symmetrical voltage was applied. Fig. 8(a) depicts the results obtained with the three-phase method and the phase angle and frequency are being



(a) Three-phase PLL



(b) Single-phase PLL

Fig. 6. The estimated pulsation and amplitude when the PLL is starting.

correctly obtained. The voltages obtained by the single-phase method are depicted in Fig. 8(b). The steady-state error on the phase angle is equal for the three phases and is caused by the phase generator. In an ideal case, the low-pass filter should result in a voltage with a phase shift of  $45^\circ$  when the cutoff frequency equals the estimated frequency. When  $v_d^s$  is not shifted  $45^\circ$  but  $(45 + \eta)^\circ$ ,  $v_d^s$  and  $v_q^s$  are then converted to the synchronous reference frame, the following equations are obtained:

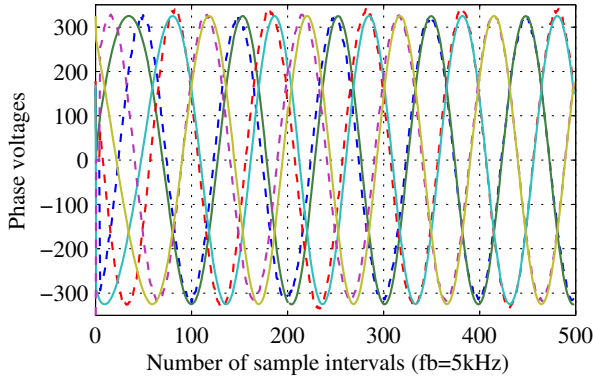
$$v_d^e = \frac{E}{2} (\cos(\theta + \hat{\theta} + \eta) + \cos(\theta - \hat{\theta}) - \cos(\theta + \hat{\theta}) + \cos(\theta - \hat{\theta} + \eta)) \quad (9)$$

$$v_q^e = \frac{E}{2} (\sin(\theta - \hat{\theta} + \eta) + \sin(\theta - \hat{\theta}) + \sin(\theta + \hat{\theta}) - \sin(\theta - \hat{\theta} + \eta).) \quad (10)$$

With the approximations:

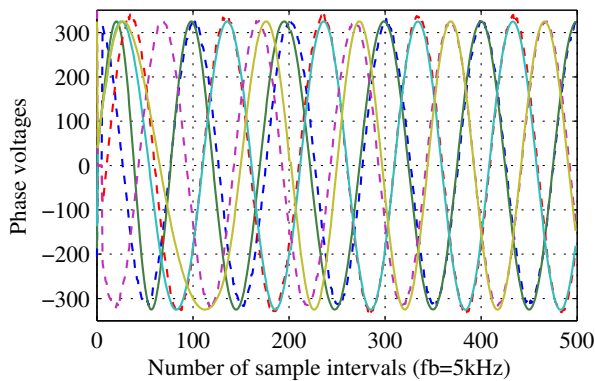
$$v_q^e = E (\theta - \hat{\theta}) - \frac{E \eta}{2} \cos(\theta + \hat{\theta} + \frac{\eta}{2}) + \frac{E \eta}{2} \quad (11)$$

The first term in (11) corresponds with (5), the second term oscillates at approximately twice the grid frequency and the last term is constant. When disregarding the second term due to the low bandwidth of the controller, the controller will regulate  $E (\theta - \hat{\theta}) + \frac{E \eta}{2}$  to zero in stead of  $E (\theta - \hat{\theta})$ . This will result in



(a) Three-phase PLL

phase of the input voltages are  $\theta_a = 0$ ,  $\theta_b = 118^\circ$  and  $\theta_c = 242^\circ$



(b) Single-phase PLL

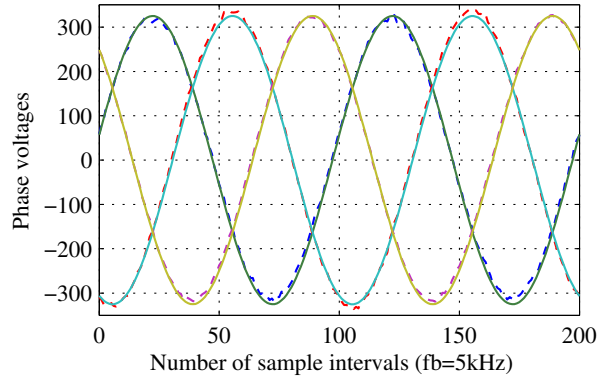
Fig. 7. The input voltage (dashed line) and calculated voltage (full line) when the PLL is starting.

the observed steady-state error which is relatively small. The three-phase SRF method does not have this problem because no filters are used to obtain the voltage in quadrature.

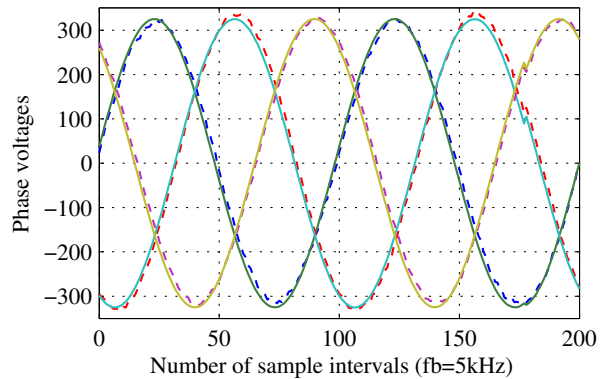
3) *Unbalanced voltages*: In the last experiment, an asymmetrical input voltage was applied. The amplitude of the three phase voltages was equal but the phase angles were  $\theta_a = 0$ ,  $\theta_b = 118^\circ$  and  $\theta_c = 242^\circ$ . Fig. 9(a) depicts the estimated amplitude and pulsation of the input voltage of the three-phase method. The oscillation in the estimated amplitude is caused by the inverse component present in the utility voltage. This oscillation can not be avoided by adding a low pass filter [7]. The single-phase method (Fig. 9(b)) shows no oscillation because the three single-phase PLL methods are not influenced by the unbalance in the input voltage. The input voltages are better estimated by the single-phase method (cf. Fig. 7(b)) compared to the three-phase method (cf. Fig. 7(a)). Using the single-phase method requires significant more calculation time compared to the three-phase method, in practice it is possible that the limits of the processor are reached when implementing three times the single-phase method.

The three-phase method requires less computational time but is sensitive to unbalance. This drawback of the three-

the



(a) Three-phase PLL



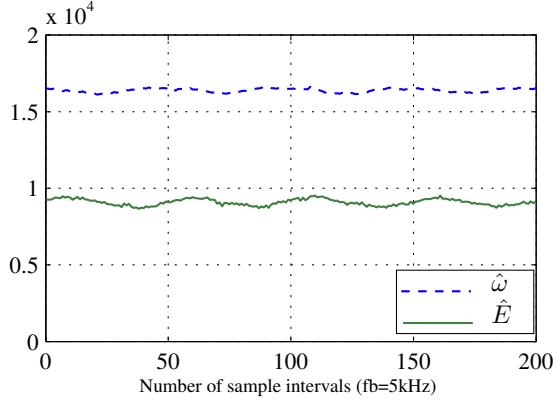
(b) Single-phase PLL

Fig. 8. The input voltages (dashed line) and calculated voltages (full line) when input voltage is three-phase symmetrical

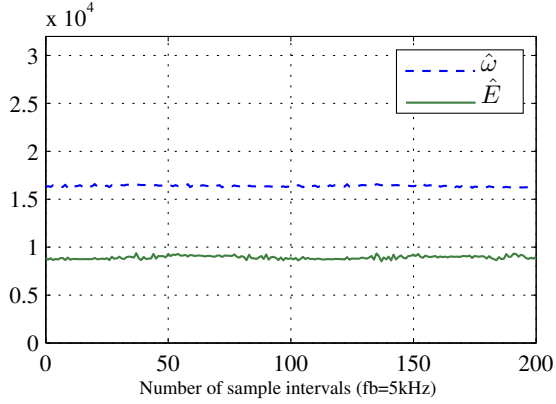
phase system can be solved by using the double synchronous reference frame PLL which is discussed in the next section.

### III. DOUBLE SYNCHRONOUS REFERENCE FRAME PLL

The double synchronous reference frame PLL was proposed in [7]. It is important that the amplitude and phase of the positive-sequence component are obtained fast and accurately, even if the utility voltage is distorted and unbalanced. This is obtained by using the following technique: an unbalanced voltage vector is defined, consisting of both positive- and negative-sequence components. The unbalanced voltage vector is expressed on the double synchronous reference frame (DSRF) in order to detect the positive-sequence component. The proposed method uses a double synchronous reference frame composed of two rotating reference axes:  $dq^{+1}$  with angular position  $\hat{\theta}$ , rotating with the positive direction and  $dq^{-1}$  with angular position  $-\hat{\theta}$ , rotating with the opposite direction.

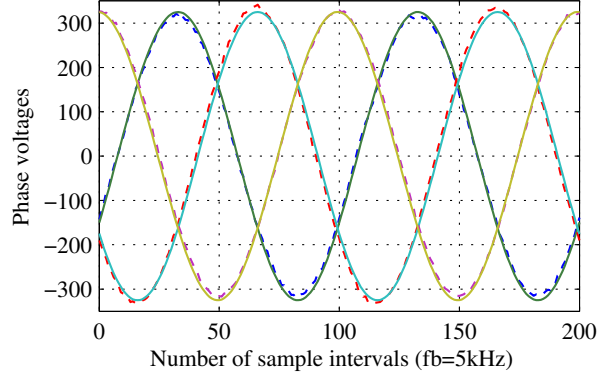


(a) Three-phase PLL

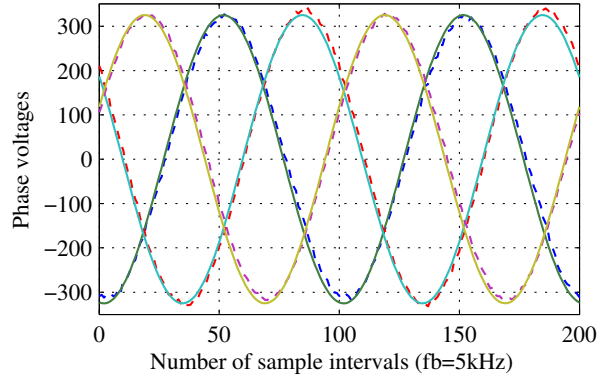


(b) Single-phase PLL

Fig. 9. The estimated pulsation and amplitude when the phase of the input voltages are  $\theta_a = 0$ ,  $\theta_b = 118^\circ$  and  $\theta_c = 242^\circ$ .



(a) Three-phase PLL



(b) Single-phase PLL

Fig. 10. The input voltage (dashed line) and calculated voltage (full line) when the phase of the input voltages are  $\theta_a = 0$ ,  $\theta_b = 118^\circ$  and  $\theta_c = 242^\circ$ .

The voltage vector  $v_s$  may be expressed on the DSRF yielding:

$$\begin{aligned}
 v_s^{dq^{+1}} &= V_s^{+1} \begin{bmatrix} \cos(\omega t - \hat{\theta}) \\ \sin(\omega t - \hat{\theta}) \end{bmatrix} + \\
 &V_s^{-1} \begin{bmatrix} \cos(-\omega t + \phi^{-1} - \hat{\theta}) \\ \sin(-\omega t + \phi^{-1} - \hat{\theta}) \end{bmatrix} \\
 v_s^{dq^{-1}} &= V_s^{+1} \begin{bmatrix} \cos(\omega t + \hat{\theta}) \\ \sin(\omega t + \hat{\theta}) \end{bmatrix} + \\
 &V_s^{-1} \begin{bmatrix} \cos(-\omega t + \phi^{-1} + \hat{\theta}) \\ \sin(-\omega t + \phi^{-1} + \hat{\theta}) \end{bmatrix}
 \end{aligned} \quad (12)$$

Equation (12) can be linearized under the following conditions:  $\sin(\omega t - \hat{\theta}) \approx \omega t - \hat{\theta}$ ,  $\cos(\omega t - \hat{\theta}) \approx 1 - \frac{(\omega t - \hat{\theta})^2}{2}$  and  $-\omega t - \hat{\theta} \approx -2 \omega t$ . Under such conditions, (12) can be

rewritten as:

$$\begin{aligned}
 v_s^{dq^{+1}} &\approx V_s^{+1} \left[ 1 - \frac{(\omega t - \hat{\theta})^2}{2} \right] + \\
 &V_s^{-1} \begin{bmatrix} \cos(-2 \omega t + \phi^{-1}) \\ \sin(-2 \omega t + \phi^{-1}) \end{bmatrix} \\
 v_s^{dq^{-1}} &\approx V_s^{+1} \begin{bmatrix} \cos(2 \omega t) \\ \sin(2 \omega t) \end{bmatrix} + \\
 &V_s^{-1} \begin{bmatrix} \cos(\phi^{-1}) \\ \sin(\phi^{-1}) \end{bmatrix} \text{ of}
 \end{aligned} \quad (13)$$

The constant values in (13) on the  $dq^{+1}$  and  $dq^{-1}$  axes correspond to the amplitude of  $v_s^{+1}$  and  $v_s^{-1}$ , while the oscillations at  $2 \omega$  correspond to the coupling between axes appearing as a consequence of the vectors rotating in opposite direction. These oscillations may be simply considered perturbations in the detection of  $v_s^{+1}$  and  $v_s^{-1}$ . The attenuation of these oscillations is achieved by means of a decoupling network, capable of obtaining accurate results for the amplitude of  $v_s^{+1}$  and  $v_s^{-1}$  while ensuring an overall improved dynamic response of the detection system. The decoupling network for decoupling the positive and negative fundamental frequency components in the  $dq^{+1}$  and  $dq^{-1}$  axes is depicted in Fig. 11.

After a stabilization period defined by the ratio between

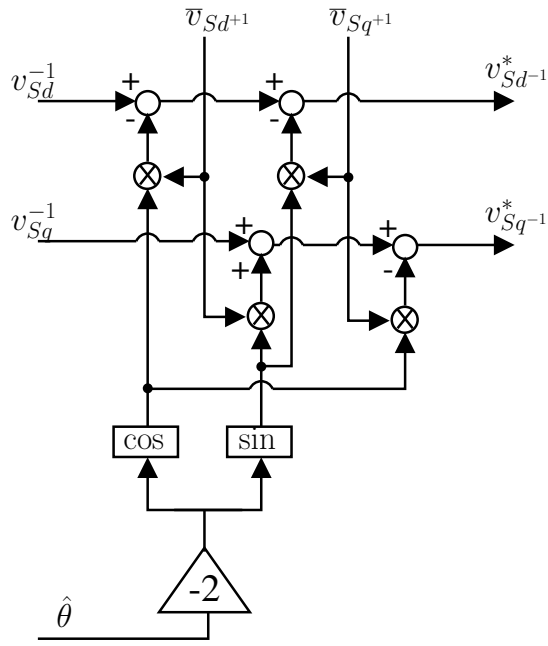


Fig. 11. Decoupling cell for canceling the effect of  $v_s^{-1}$  on the  $dq^{+1}$  frame signals

the cut-off frequency of the LPF and the utility fundamental frequency, the amplitude  $v_s^{+1}$  may be finally determined.

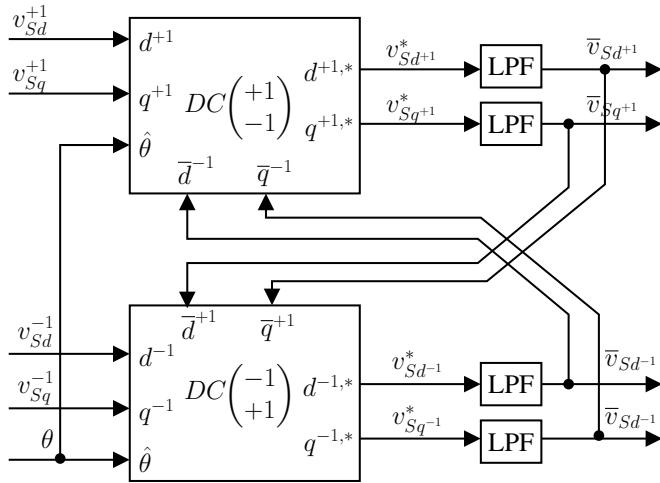


Fig. 12. Decoupling network of  $dq^{+1}$  and  $dq^{-1}$  reference frames

The block diagram of the DDSRF-PLL is shown in Fig. 13. Its performance improvement comes from the decoupling network added to the DSRF. The DDSRF-PLL can achieve high precision to detect the phase [7].

#### IV. CONCLUSION

In this paper three commonly known PLL methods are discussed and two methods were experimentally verified and tested in case of voltage unbalance and transients. The single-phase SRF method is not influenced by unbalance in the

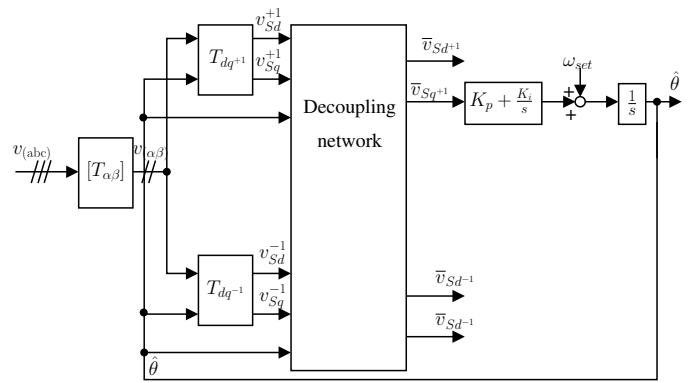


Fig. 13. Block diagram of the DDSRF-PLL

input voltage, a disadvantage of this method is the need for extra computational time. The three-phase method requires less computational time but is sensitive to unbalance. This drawback of the three-phase system can be solved by using the double synchronous reference frame PLL which is presented in this paper.

#### ACKNOWLEDGMENT

The work of B. Meersman is carried out in the frame of the FWO Project (G.0587.07N). The work of T.L. Vandoorn is supported by a Ph.D. fellowship from FWO-Vlaanderen (Research Foundation - Flanders, Belgium). The research was carried out in the frame of the inter-university Attraction poles IAP-VI-021, funded by the Belgian Government.

#### REFERENCES

- [1] G. Xiaoqiang, W. Weiyang, S. Xiaofeng, and S. Guocheng, "Phase locked loop for electronically-interfaced converters in distributed utility network," in *Proceedings of the International Conference on Electrical Machines and Systems (ICEMS 2008)*, Oct.17-20 2008, pp. 2346-2350.
- [2] J.-W. Choi, Y.-K. Kim, and H.-G. Kim, "Digital PLL control for single-phase photovoltaic system," *IEE Proc.-Electr. Power Appl.*, vol. 153, no. 1, pp. 40-46, Jan. 2006.
- [3] S.-K. Chung, "A phase tracking system for three phase utility interface inverters," *IEEE Trans. Power Electron.*, vol. 15, no. 3, pp. 431-438, May 2000.
- [4] —, "Phase-locked loop for grid-connected three-phase power conversion systems," *IEE Proceedings-Electric Power Applications*, vol. 147, no. 3, pp. 213-219, May 2000.
- [5] V. Kaura and V. Blasko, "Operation of a phase locked loop system under distorted utility conditions," *IEEE Trans. Ind. Appl.*, vol. 33, no. 1, pp. 58-63, Jan. 1997.
- [6] J. Rodríguez, J. Pontt, C. A. Silva, P. Correa, P. Lezana, P. Cortés, and U. Ammann, "Predictive current control of a voltage source inverter," *IEEE Trans. Ind. Appl.*, vol. 54, no. 1, pp. 495-503, Feb. 2007.
- [7] P. Rodríguez, J. Pou, J. Bergas, J. I. Candela, R. P. Burgos, and D. Boroyevich, "Decoupled double synchronous reference frame PLL for power converters control," *IEEE Trans. Power Electron.*, vol. 22, no. 2, pp. 584-592, Mar. 2007.